

# Connecting the physical properties of galaxies with the overdensity and tidal shear of the large-scale environment

Jounghun Lee<sup>1\*</sup>, and Cheng Li<sup>2,3</sup>

<sup>1</sup>*Department of Physics and Astronomy, FPRD, Seoul National University, Seoul 151-747, Korea*

<sup>2</sup>*Max-Planck-Institute for Astrophysics, Karl-Schwarzschild-Str. 1, D-85741 Garching, Germany*

<sup>3</sup>*MPA/SHAO Joint Center for Astrophysical Cosmology at Shanghai Astronomical Observatory, Nandan Road 80, Shanghai 200030, China*

Accepted 2008 ???. Received 2008 ???; in original form 2008 March 1

## ABSTRACT

We have examined the correlations between the large-scale environment of galaxies and their physical properties, using a sample of 28,354 nearby galaxies drawn from the Sloan Digital Sky Survey, and the large-scale tidal field reconstructed in real space from the 2Mass Redshift Survey and smoothed over a radius of  $\sim 6h^{-1}$  Mpc. The large-scale environment is expressed in terms of the overdensity, the ellipticity of the shear and the type of the large-scale structure. The physical properties analyzed include  $r$ -band absolute magnitude  $M_{0.1r}$ , stellar mass  $M_*$ ,  $g-r$  colour, concentration parameter  $R_{90}/R_{50}$  and surface stellar mass density  $\mu_*$ .

Both luminosity and stellar mass are found to be statistically linked to the large-scale environment, regardless of how the environment is quantified. More luminous (massive) galaxies reside preferentially in the regions with higher densities, lower ellipticities and halo-like structures. At fixed luminosity, the large-scale overdensity depends strongly on parameters related to the recent star formation history, that is colour and  $D(4000)$ , but is almost independent of the structural parameters  $R_{90}/R_{50}$  and  $\mu_*$ . All the physical properties are statistically linked to the shear of the large-scale environment even when the large-scale density is constrained to a narrow range. This statistical link has been found to be most significant in the quasi-linear regions where the large-scale density approximates to an order of unity, but no longer significant in highly nonlinear regimes with  $\delta_{LS} \gg 1$ .

Our results suggest that the initial conditions have made nonnegligible contributions to establishing the environmental dependence of galaxy properties. It is expected that our results may give a new clue to the unknown physical mechanism of the galaxy-environment relationships.

**Key words:** methods:statistical – galaxies:clustering – large-scale structure of Universe – cosmology:theory

## 1 INTRODUCTION

The spatial distribution of galaxies as a function of their physical properties provides important constraints on models of galaxy formation. Our understanding of such distribution has come primarily from large redshift surveys of nearby galaxies, for example the Sloan Digital Sky Survey (SDSS; York et al. 2000). These surveys have shown that galaxies are not distributed homogeneously, but in filamentary structures that surround large empty regions, or voids. More importantly, galaxies of different properties are found to be associated with different environments. Indeed, galaxy

properties such as morphology, luminosity, colour, surface brightness, gas content, mean stellar age, star formation rate, and nuclear activity are all correlated with the overdensity of the galaxy environment (Oemler 1974; Dressler 1980; Postman & Geller 1984; Whitmore et al. 1993; Balogh et al. 2001; Lewis & et al. 2002; Martínez et al. 2002; Gomez et al. 2003; Goto et al. 2003; Hogg et al. 2003; Kauffmann et al. 2004; Blanton et al. 2005; Rojas et al. 2005; Park et al. 2007). Galaxy colour is found to be the galaxy property most predictive of the local density (Kauffmann et al. 2004; Blanton et al. 2005), while colour and luminosity jointly comprise the most predictive pair of properties (Blanton et al. 2005).

\* E-mail:jounghun@astro.snu.ac.kr

Studies of galaxy clustering, usually quantified by

two-point correlation function (2PCF), have also found different clustering amplitudes for different types of galaxies (e.g. Davis & Geller 1976; Mo, McGaugh, & Bothun 1994; Park et al. 1994; Norberg et al. 2001, 2002; Budavári et al. 2003; Madgwick et al. 2003; Zehavi et al. 2002; Zehavi et al. 2005; Li et al. 2006). These studies have revealed that the galaxies with higher luminosities, higher stellar masses, red colours, bulge-dominated morphologies and spectral types indicative of old stellar populations reside preferentially in the dense regions.

Although the physical mechanism for the environmental dependence of galaxy properties has yet been fully understood, numerical simulations and (semi-)analytical work have led us to bring up a standard picture, according to which the nonlinear processes on small scales like hierarchical merging, galaxy interactions, and tidal forces have nurtured the environment-galaxy property relations. However, it has been realized from recent observational studies that the large-scale distribution of galaxies may be also correlated with their physical properties. For instance, Li et al. (2006) found that, at *fixed* stellar mass, the dependence of clustering on colour and 4000-Å break strength — measures of mean stellar age — extends over very large physical scales up to 10 Mpc or more. This is rather surprising, because these scales are significantly larger than those of individual dark matter haloes over which different galaxies could have exerted any influence on each other on a Hubble timescale. What this implies is that, the star formation history of a galaxy is somehow imprinted at birth. It is then natural to speculate that the role of the initial cosmological conditions in establishing the environmental variations of galaxy properties is a missing piece in the standard picture (see also, Tanaka et al. 2004).

In order to find clear observational evidence in support of this hypothesis, it is necessary to extend the previous studies not only by going to large scales, but also by quantifying the galaxy environment in a more explicit manner. In previous studies, the environment is usually expressed in terms of overdensities in galaxy number that are estimated in a fixed sphere/aperture centered on the galaxies being studied. The radius of the sphere/aperture is chosen to be  $\lesssim$  a few Mpc, as to probe the physical processes occurring inside individual dark matter haloes. Compared to the local density, the 2PCF is more powerful in the sense that it encapsulates information about how galaxy properties depend on the overdensity of the galaxy environment over a wide range of physical scales. However, it doesn't account for the other aspects of the large-scale environment, such as the *tidal shear*. This is important given the filamentary distribution of galaxies on large scales, which is in fact a nonlinear manifestation of the primordial tidal field (Bond et al. 1996).

The morphology-density relation is one of the most fundamental correlations between the properties galaxies and the local environment. Recently, Lee & Lee (2008) have extended the quantification of this relation to large scales, using a sample of 15,882 nearby galaxies from the Tully Catalogue that have been well-determined in morphological type, and the overdensity and tidal shear of the real-space linear density field reconstructed from the 2Mass Redshift Survey (2MRS) and smoothed with a Wiener filter on a radius of  $\approx 6h^{-1}$ Mpc. The authors found that the galaxy morpholog-

ical type is a strong function of not only the overdensity but also the tidal shear of the large-scale environment.

As pointed out by Li et al. (2006), the standard morphological classification scheme mixes elements that depend on the structure of a galaxy with elements related to its recent star formation history, and so it is by no means that these two elements should depend on environment in the same way. In this paper, we extend the study of Lee & Lee (2008) by using a sample of galaxies drawn from the SDSS and investigating the dependence of the large-scale overdensity and tidal shear on a variety of physical properties, including colour ( $g - r$ ), 4000-Å break strength ( $D(4000)$ ), concentration parameter ( $R_{90}/R_{50}$ ) and stellar surface mass density ( $\mu_*$ ). The first two quantities, that is,  $g - r$  and  $D(4000)$ , are parameters associated with the recent star formation history of the galaxy, whereas the other two are related to galaxy structure. We also probe the dependence on luminosity and stellar mass. In future studies, we plan to examine with more physical properties such as star formation rate and nuclear activity.

The structure of this paper is as follows. In Section 2 we give a brief overview of the observational data, and explain how to define the shear of large-scale environment at the positions of the SDSS galaxies. We present the observed links of the galaxy properties to the density and to the shear of the large-scale environment in Sections 3 and 4, respectively. In Section 5 we show how the galaxy properties vary with the types of the large-scale structures in which they are found. In Section 6 we summarize the results and draw a final conclusion.

We assume a cosmological model with the density parameter  $\Omega_0 = 0.3$  and the cosmological constant  $\Lambda_0 = 0.7$ . To avoid the  $-5 \log_{10} h$  factor, the Hubble's constant  $h = 1$ , in units of  $100 \text{ km s}^{-1} \text{ Mpc}^{-1}$ , is assumed throughout this paper when computing absolute magnitudes.

## 2 DATA

### 2.1 The SDSS galaxies and physical quantities

The galaxy sample analyzed in this study is constructed from the SDSS. The survey goals are to obtain photometry of a quarter of the sky and spectra of nearly one million objects. Imaging is obtained in the  $u$ ,  $g$ ,  $r$ ,  $i$ ,  $z$  bands (Fukugita et al. 1996; Smith et al. 2002; Ivezić et al. 2004) with a special purpose drift scan camera (Gunn et al. 1998) mounted on the SDSS 2.5 meter telescope (Gunn et al. 2006) at Apache Point Observatory. The imaging data are photometrically (Hogg et al. 2001; Tucker et al. 2006) and astrometrically (Pier et al. 2003) calibrated, and used to select spectroscopic targets for the main galaxy sample (Strauss et al. 2002), the luminous red galaxy sample (Eisenstein et al. 2001), and the quasar sample (Richards et al. 2002). Spectroscopic fibres are assigned to the targets using an efficient tiling algorithm designed to optimise completeness (Blanton et al. 2003c). The details of the survey strategy can be found in York et al. (2000) and an overview of the data pipelines and products is provided in the Early Data Release paper (Stoughton et al. 2002). More details on the photometric pipeline can be found in Lupton et al. (2001).

Our parent sample for this study consists of 397,344 objects that are spectroscopically classified as galaxies and have data publicly available in the SDSS Data Release Four (DR4; Adelman-McCarthy et al. 2006). These galaxies have Petrosian  $r$ -band magnitudes in the range  $14.5 < r < 17.77$  after correction for foreground galactic extinction using the reddening maps of Schlegel et al. (1998) and have redshifts in the range  $0.005 \lesssim z < 0.30$ , with a median  $z$  of 0.10. In order to have a similar redshift distribution as the 2MRS, we have selected the galaxies with  $z \leq 0.04$ . We also restrict the galaxies to the apparent magnitude range  $14.5 < r < 17.6$ , as to yield a uniform galaxy sample that is complete over the entire area of the survey, as well as to the absolute magnitude range  $-23 < M_{0.1r} < -17$ . Here,  $M_{0.1r}$  is the  $r$ -band absolute magnitude corrected to its  $z = 0.1$  value using the  $K$ -correction code of Blanton et al. (2003a) and the luminosity evolution model of Blanton et al. (2003b). The resulting sample includes a total of 28,354 galaxies with a median redshift of  $\langle z \rangle \approx 0.02$ .

The galaxies are then divided into a variety of different subsamples according to their physical parameters, including absolute magnitude ( $M_{0.1r}$ ), stellar mass ( $M_*$ ), colour  $[(g-r)_{0.1}]$ , 4000-Å break strength ( $D(4000)$ ), concentration ( $R_{90}/R_{50}$ ) and stellar surface mass density ( $\mu_*$ ). Here,  $(g-r)_{0.1}$  is the  $g-r$  colour corrected to its  $z = 0.1$  value using the  $K$ -correction code of Blanton et al. (2003a).  $D(4000)$  is the narrow version of the index defined in Balogh et al. (1999).  $R_{90}$  and  $R_{50}$  are the radii enclosing 90 and 50 per cent of the galaxy light in the  $r$  band (see Stoughton et al. 2002). The half-light radius in the  $z$  band and the stellar mass yield the effective stellar surface mass density ( $\mu_* = M_*/2\pi r_{50,z}^2$ , in units of  $h^2 M_\odot \text{kpc}^{-2}$ ). The stellar masses of galaxies are estimated using their spectra, and they are publicly available at <http://www.mpa-garching.mpg.de/SDSS>. The reader is referred to Kauffmann et al. (2003) and Brinchmann et al. (2004) for details.

## 2.2 The large-scale density and shear field

Now that the galaxy sample is constructed, we would like to measure the large-scale shear at the locations of the sample galaxies. Erdođdu et al (2006) has reconstructed the real space density and velocity fields smoothed on the scale of  $\approx 6h^{-1}\text{Mpc}$ , in a cubic consisting of  $64^3$  pixel points with linear size of  $400h^{-1}\text{Mpc}$ , by applying the wiener filter technique to the galaxy catalogs from the fully-sky 2Mass Redshift Survey (2MRS). Lee & Erdođdu (2007) have used this real-space 2MRS density field to reconstruct the tidal shear field. Basically, they performed the Fourier transformation of the real-space density field  $\delta(\mathbf{x})$  calculated the Fourier space tidal field as  $T_{ij}(\mathbf{k}) = k_i k_j \delta(\mathbf{k})/k^2$ . Then, they perform the inverse Fourier transformation of the Fourier space tidal field to derive the real space tidal field,  $T_{ij}(\mathbf{x})$ .

By applying the cloud-in-cell method to the 2MRS tidal field reconstructed by Lee & Erdođdu (2007), we calculate the tidal shear tensor at the position of each selected SDSS galaxy. We determine the three dimensional positions of the selected galaxies from the given information on  $z$ ,  $\delta$  and  $\alpha$ , assuming a  $\Lambda\text{CDM}$  cosmology of  $\Omega_m = 0.3$ ,  $\Omega_\Lambda = 0.7$  and  $h = 1$ . After measuring the tidal tensor at each galaxy position, we diagonalize it to find its three eigenvalues,  $\{\lambda_1, \lambda_2, \lambda_3\}$ , (with  $\lambda_1 \geq \lambda_2 \geq \lambda_3$ ). The trace of the

tidal tensor at the position of a given galaxy equals the linear density contrast of the large-scale environment ( $\delta_{\text{LS}}$ ) in which the given galaxy is embedded:

$$\delta_{\text{LS}} \equiv \lambda_1 + \lambda_2 + \lambda_3. \quad (1)$$

The shear of the large scale environment is defined as the ellipticity of the gravitational potential ( $e_{\text{LS}}$ ) (Bardeen et al. 1986) as

$$e_{\text{LS}} \equiv \frac{\lambda_1 - \lambda_3}{2\delta_{\text{LS}}}. \quad (2)$$

We calculate the large scale density ( $\delta_{\text{LS}}$ ) and shear ( $e_{\text{LS}}$ ) at the positions of the selected SDSS galaxies by eqs. [1] and [2].

## 3 CORRELATION OF THE LARGE-SCALE OVERDENSITY WITH GALAXY PROPERTIES

In this section we study how the overdensity of the large-scale environment of galaxies depends on their physical properties.

We first divide the SDSS galaxy sample described in § 2.1 into four subsamples according to absolute magnitude  $M_{0.1r}$ , as well as four subsamples according to stellar mass  $\log(M_*/M_\odot)$ . Table 1 lists the ranges of  $M_{0.1r}$  and  $\log(M_*/M_\odot)$  for these subsamples, which are chosen in such a way that each subsample has approximately the same number of galaxies. For each subsample, we then calculate the mean value of  $\delta_{\text{LS}}$ , the overdensity of the large-scale environment (see § 2.2). Fig. 1 plots  $\delta_{\text{LS}}$  as histograms, as function of the mean absolute magnitude (upper panel) and stellar mass (lower panel) of the subsamples. The errors are calculated as  $\sigma/\sqrt{N_g}$  where  $\sigma$  is one standard deviation of  $\delta_{\text{LS}}$  and  $N_g$  is the number of the galaxies belonging to a given subsample. The average result of the whole sample is plotted as a dotted line in both panels.

As can be seen from Fig. 1, both luminosity and stellar mass are statistically linked to the large-scale density, that is, the mean value of the overdensity,  $\langle \delta_{\text{LS}} \rangle$ , increases with increasing luminosity and stellar mass. It is interesting to notice that the trend of  $\langle \delta_{\text{LS}} \rangle$  with  $\log(M_*/M_\odot)$  is stronger than the trend with  $M_{0.1r}$ . This suggests that stellar mass is more susceptible to the effect of the density of large-scale environment.

Next, we study the dependence of  $\langle \delta_{\text{LS}} \rangle$  on the other four physical quantities:  $(g-r)_{0.1}$ ,  $D(4000)$ ,  $R_{90}/R_{50}$  and  $\mu_*$ . Since all these quantities are correlated with galaxy luminosity and stellar mass, we have restricted this analysis to the third luminosity subsample (Sample III) in Table 1. The results are plotted in Fig. 2. Each panel corresponds to one physical quantity, according to which all the galaxies in Sample III are divided further into four subsamples in the same way as described above. Details of these subsamples are given in Table 2.

It is seen that the large-scale overdensity  $\langle \delta_{\text{LS}} \rangle$  depends strongly on parameters related to recent star formation history, that is,  $(g-r)_{0.1}$  and  $D(4000)$ , but very weakly on structural parameters  $R_{90}/R_{50}$  and  $\mu_*$ . ‘‘Old’’ galaxies with redder colours and higher values of  $D(4000)$  are preferentially located in the large-scale environment of

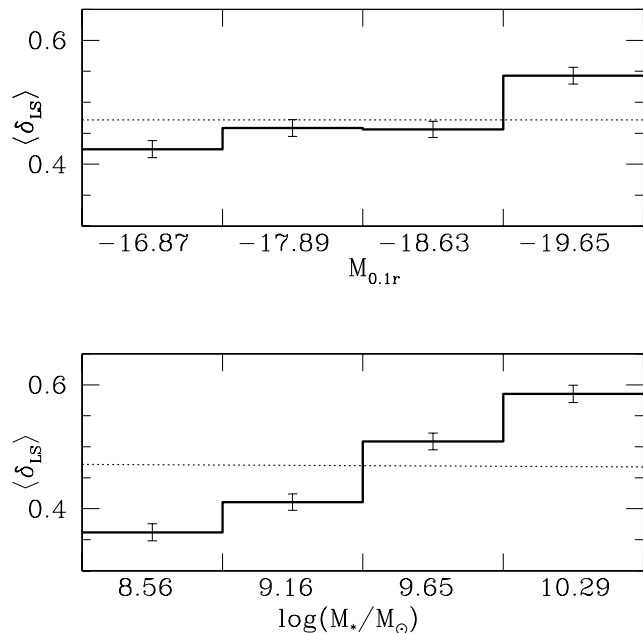


**Figure 1.** Mean of the large scale density ( $\delta_{LS}$ ) averaged over four different samples of the SDSS galaxies divided by their r-band absolute magnitude (upper) and stellar mass (lower).

**Table 1.** The range of the r-band absolute magnitude, the stellar mass, the specific star formation rate, and the  $H_\alpha$ -emission line of the SDSS galaxies belonging to each subsample

Sample	$M_{0.1r}$	$\log[M_*/M_\odot]$
I	$> -17.5$	$< 8.9$
II	$[-18.2, -17.5]$	$[8.9, 9.4]$
III	$[-19.1, -18.2]$	$[9.4, 10.0]$
IV	$< -19.1$	$> 10.0$

higher densities, with the colour ( $D(4000)$ ) dependence becoming more remarkable for the galaxies with  $(g-r)_{0.1} \gtrsim 0.7$  ( $D(4000) \gtrsim 1.5$ ). These results are in good agreement with Li et al. (2006). We would like to point out that the weak trends of  $\langle \delta_{LS} \rangle$  with  $R_{90}/R_{50}$  and  $\mu_*$  seen from the bottom panels of Fig. 2 probably follow from the trends with luminosity and stellar mass as seen from Fig. 1, since the luminosity range of Sample III in Table 1 may be not narrow enough. We would come back to this point in future with larger samples.

**Table 2.** The range of  $(g-r)_{0.1}$ ,  $D(4000)$ ,  $R_{90}/R_{50}$ , and  $\log \mu_*$  of the SDSS galaxies belonging to each subsample with the constraint of  $9.4 \leq \log(M_*/M_\odot) \leq 10.0$

Sample	$(g-r)_{0.1}$	$D(4000)$	$R_{90}/R_{50}$	$\log \mu_*$
I	$< 0.42$	$< 1.25$	$< 2.18$	$< 8.30$
II	$[0.42, 0.53]$	$[1.25, 1.34]$	$[2.18, 2.40]$	$[8.30, 8.57]$
III	$[0.53, 0.69]$	$[1.34, 1.52]$	$[2.40, 2.65]$	$[8.57, 8.88]$
IV	$> 0.69$	$> 1.52$	$> 2.65$	$> 8.88$

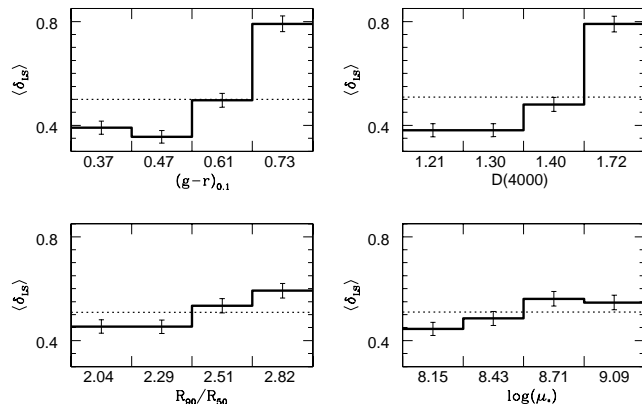
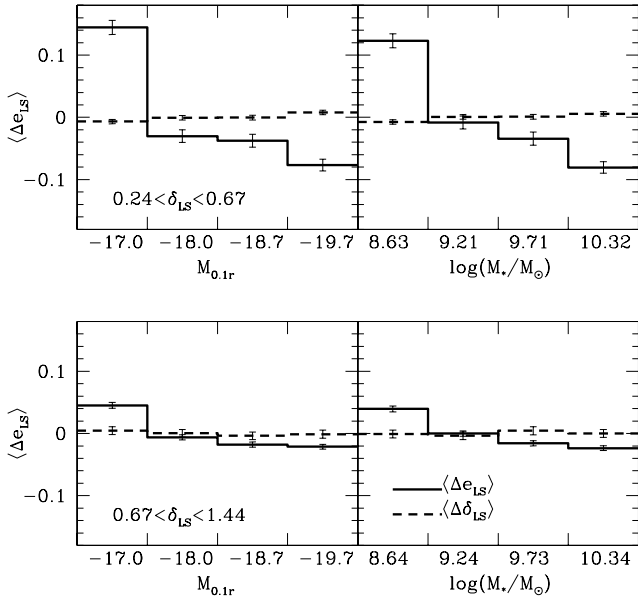


**Figure 2.** Mean of the large scale density ( $\delta_{LS}$ ) averaged over four different samples of the SDSS galaxies divided by their  $g-r$  color (top-left), 4000-Å break strength (top-right), concentration parameter (bottom-left) and surface stellar mass density (bottom-right) from SDSS DR4.

#### 4 CORRELATION OF THE LARGE-SCALE TIDAL SHEAR WITH GALAXY PROPERTIES

In this section we explore the dependence of the large-scale *tidal shear* on the same set of physical properties as in the previous section. In order to normalize out the dependence of large-scale overdensity on these properties, we have divided all the galaxies into a number of subsamples with the large-scale overdensity limited to a narrow range. Such density constrains can also break the degeneracy between the trends with galaxy luminosity and stellar mass and the trends with the other properties. Selecting only those galaxies which are located in the regions whose large-scale density falls in a fixed range, we divide these galaxies into four subsamples by binning their galaxy properties in the same way as in § 2, and calculate the mean value of  $\Delta e_{LS}$  averaged over each subsample. Here,  $\Delta e_{LS}$  is defined as  $\Delta e_{LS} \equiv e_{LS} - \bar{e}_{LS}$  where  $\bar{e}_{LS}$  is the global mean of  $e_{LS}$  averaged over all the selected galaxies. The results are shown in Figs. 3-5.

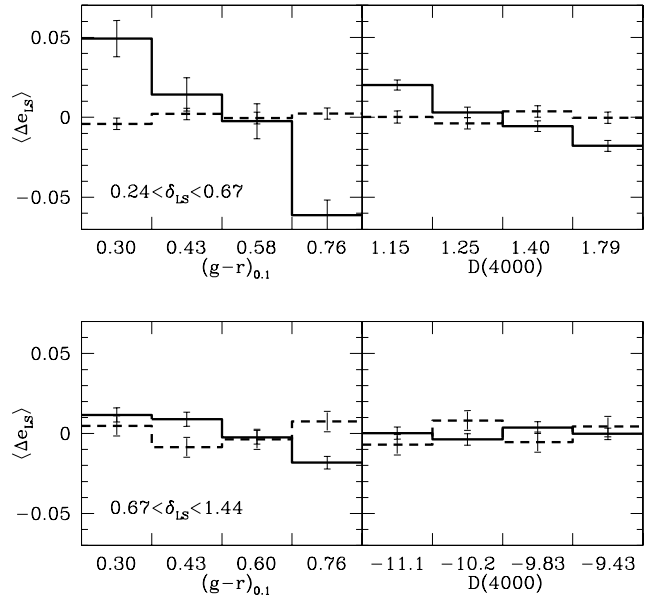
Fig 3 plots as solid histograms the mean value of  $\Delta e_{LS}$  for the subsamples selected according to  $M_{0.1r}$  (left) and  $\log(M_*/M_\odot)$  (right), and for overdensity constrained to the range of  $0.24 \leq \delta_{LS} \leq 0.67$  (top) and  $0.67 \leq \delta_{LS} \leq 1.44$  (bottom). We consider only these two ranges of  $\delta_{LS}$  since in the other ranges of  $\delta_{LS} \leq 0.67$  and  $\delta_{LS} \geq 1.14$ , the number of the galaxies are too small to yield reliable statistics. As can be seen, the value of  $\langle \Delta e_{LS} \rangle$  also varies significantly with  $M_{0.1r}$  and  $\log(M_*/M_\odot)$  in the density range of  $0.24 \leq \delta_{LS} \leq 0.67$ . In the other range of  $0.67 \leq \delta_{LS} \leq 1.14$ , the variation of  $\langle \Delta e_{LS} \rangle$  is weaker but still exists to a nonnegligible degree, that is, more luminous galaxies are preferentially located in the regions with lower ellipticity. To examine whether or not the effect of the large-scale density has been removed from the signals, the value of  $\langle \Delta \delta_{LS} \rangle$  is also plotted as dashed histogram in each panel. As can be seen, the values of  $\langle \Delta \delta_{LS} \rangle$  are close to zero for all luminosities and all stellar masses, indicating that the observed variations of  $\langle \Delta e_{LS} \rangle$  between the subsamples are not due to the effect of the large-scale density.



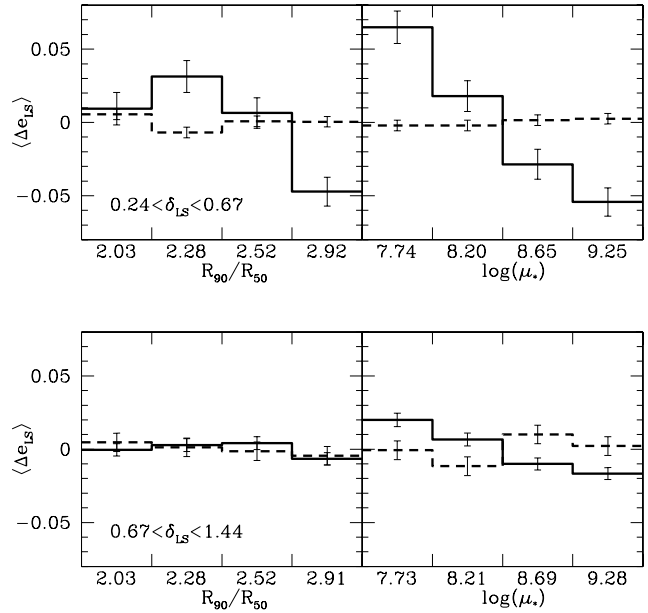
**Figure 3.** Mean of the large-scale shear difference ( $\Delta e_{LS} \equiv e_{LS} - \bar{e}_{rmLS}$ ) averaged over four different samples of the SDSS galaxies (solid histogram) divided by their r-band absolute magnitude (left), stellar mass (right). The errors are calculated as one standard deviation in the measurement of the mean values. The large scale density is confined to a narrow range:  $0.24 < \delta_{LS} < 0.67$  (top) and  $0.67 < \delta_{LS} < 1.44$  (bottom). In each panel, the dashed histogram represents the mean of the large-scale density difference averaged over the four subsamples with the density constrained to the same range.

Fig 4 plots the same thing as Fig 3 but the four subsamples are selected to  $(g-r)_{0.1}$  (left) and  $D(4000)$  (right). As can be seen, the value of  $\langle \Delta e_{LS} \rangle$  also varies significantly with  $(g-r)_{0.1}$  when the density range is limited to a narrow range of  $0.24 \leq \delta_{LS} \leq 0.67$ . The dependence on  $D(4000)$  is weaker than that on colour, but is still significant. The galaxies with redder colour or higher value of  $D(4000)$  are preferentially located in the large-scale environment with lower ellipticities. In the higher density range of  $0.67 \leq \delta_{LS} \leq 1.14$ , the variation of  $\langle \Delta e_{LS} \rangle$  is quite weak, almost negligible.

Fig 5 shows the results for the four subsamples selected according to concentration parameter  $R_{90}/R_{50}$  (left) and surface stellar mass density  $\log \mu_*$  (right). As can be seen, the value of  $\langle \Delta e_{LS} \rangle$  also varies significantly with  $\log \mu_*$  when the density range is given as  $0.24 \leq \delta_{LS} \leq 0.67$ , whereas the dependence on  $R_{90}/R_{50}$  is much weaker. This indicates that the surface mass density is more susceptible to the effect of the large-scale shear. The galaxies with high surface stellar mass density are preferentially located in the large-scale environment with low ellipticities. In the higher density range of  $0.67 \leq \delta_{LS} \leq 1.14$ , the variation of  $\langle \Delta e_{LS} \rangle$  is almost negligible.



**Figure 4.** Same as Fig. 3 but the subsamples constructed according to the  $(g-r)$  color (left) and the 4000-Å break strength (right)



**Figure 5.** Same as Fig. 3 but the subsamples constructed according to the concentration parameter (left) and the surface stellar mass density (right)

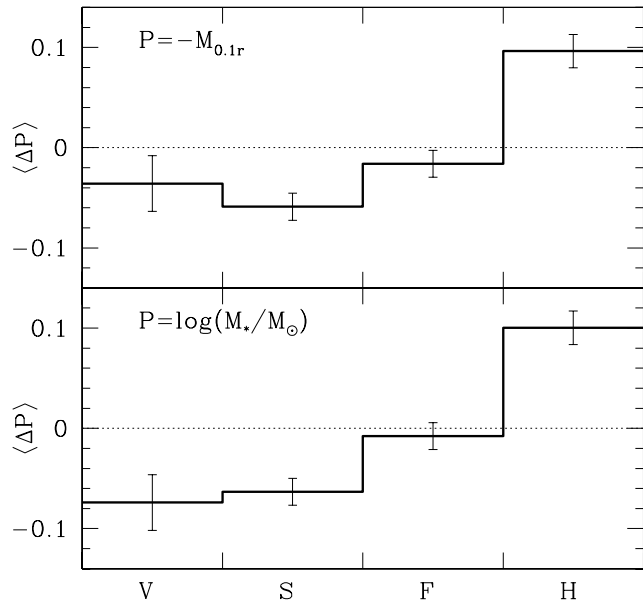


**Figure 6.** Mean values of the r-band absolute magnitude (top) and stellar mass (bottom) of the SDSS galaxies located in the voids (V), the sheets (S), the filaments (F) and the halos (H), relative to the global mean values averaged over the whole galaxy sample.

## 5 VARIATION WITH THE LARGE SCALE STRUCTURE

Another interesting issue to address is the dependence of the properties of galaxies on the type of the large scale structure (LSS) where the galaxies are found. To classify the type of LSS, we consider the signs of the three eigenvalues,  $\lambda_1$ ,  $\lambda_2$ ,  $\lambda_3$  of the tidal shear tensor at the location of a given galaxy. We use the following criteria to classify the given region into a void, a sheet, a filament and a halo.

$$\text{void} \quad \text{if } \lambda_1 < 0, \quad (3)$$

$$\text{sheet} \quad \text{if } \lambda_1 > 0 \ \& \ \lambda_2 < 0, \quad (4)$$

$$\text{filament} \quad \text{if } \lambda_2 > 0 \ \& \ \lambda_3 < 0, \quad (5)$$

$$\text{halo} \quad \text{if } \lambda_3 > 0 \quad (6)$$

Table 3 lists the mean value of the large-scale density ( $\bar{\delta}_{LS}$ ) and the total number of the galaxies ( $N_g$ ) located in the void (V), sheet (S), filament (F) and halo (H).

In Fig. 6, we show the relative mean values of r-band absolute magnitude (top) and stellar mass (bottom) for the galaxies located in voids, sheets, filaments and haloes separately. Here,  $\Delta P$  is defined as  $\Delta P \equiv P - \bar{P}$  where  $P$  represents the value of the physical quantity and  $\bar{P}$  is the mean of  $P$  averaged over the whole galaxy sample. We see that the most luminous (massive) galaxies are found in halo-like structures, whereas the least luminous galaxies are located in voids.

Fig. 7 shows how the average of the other four physical parameters,  $(g-r)_{0.1}$ ,  $D(4000)$ ,  $R_{90}/R_{50}$  and  $\mu_*$ , relative to their global means averaged over the whole galaxy sample changes among different types of the surrounding

**Table 3.** The LSS type, the mean of the large scale density, and the total number of the SDSS galaxies

Sample	LSS-Type	$\bar{\delta}_{LS}$	$N_g$
V	Void	$-0.846 \pm 0.005$	1919
S	Sheet	$-0.395 \pm 0.004$	8797
F	Filament	$0.457 \pm 0.005$	9892
H	Halo	$1.800 \pm 0.013$	7746

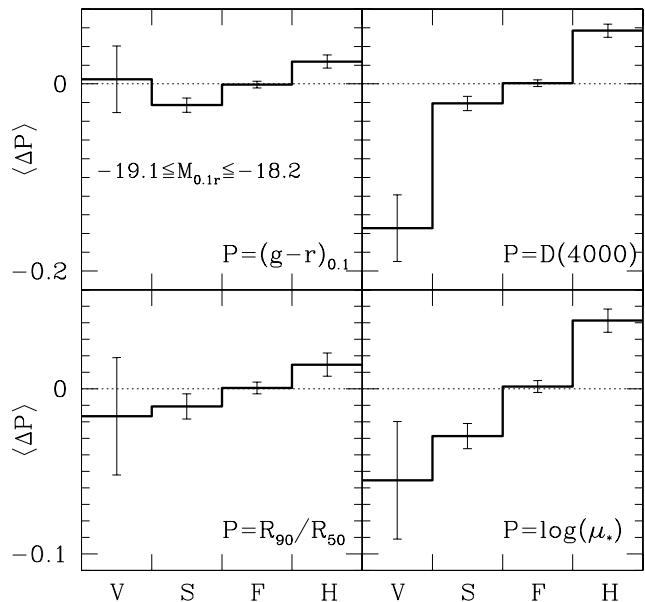


**Figure 7.** Relative mean values of the  $(g-r)$  color (top-left), 4000-Å break strength (top-right), concentration parameter (bottom-left), surface stellar mass density (bottom-right) of the SDSS galaxies with absolute r-band magnitude in the range of  $[-19.1, -18.2]$ , located in the voids (V), the sheets (S), the filaments (F) and the halos (H).

LSS. The analysis is performed only for the third luminosity subsample (Sample III) in Table 1 to remove the effect of density-galaxy property relations. We see that the variation of  $D(4000)$  and  $\mu_*$  with the type of LSS is quite significant. The mean values of  $D(4000)$  and  $\mu_*$  are highest in halos and lowest in voids. Whereas the mean values of  $(g-r)_{0.1}$  and  $R_{90}/R_{50}$  depend only weakly on the types of LSS. It suggests that the quantities,  $D(4000)$  and  $\mu_*$  are better indicators of the relation with the types of LSS.

## 6 SUMMARY AND CONCLUSION

By using a sample of low- $z$  galaxies drawn from the Sloan Digital Sky Survey and the large-scale tidal field reconstructed in real space from the 2Mass Redshift Survey, we have studied the relationships between the large-scale environment of galaxies and their physical properties. The large-scale environment is expressed in terms of the overdensity, the ellipticity of the shear and the type of the large-scale structure. The physical properties analyzed here include the

$r$ -band absolute magnitude, the stellar mass, the concentration parameter and the surface stellar mass density.

Our results can be summarized as follows.

- Both luminosity and stellar mass are found to be statistically linked to the large-scale environment, regardless of how the environment is quantified. More luminous (massive) galaxies reside preferentially in the regions with higher densities, lower ellipticities and halo-like structures.
- At fixed luminosity, the large-scale overdensity depends strongly on parameters related to the recent star formation history, that is colour and 4000-Å break strength, but is almost independent of the structural parameters, concentration and surface stellar mass density. This is well consistent with the findings of Li et al. (2006).
- All the physical properties considered here are statistically linked to the shear of the large-scale environment even when the large-scale density is constrained to a narrow range. Galaxies with red colours, high values of  $D(4000)$ , concentrated morphology and high surface stellar mass density tend to be located in low-ellipticity regions. This statistical link has been found to be most significant in the quasi-linear regions where the large-scale density is approximately an order of unity:  $\delta_{LS} \sim 1$ . In highly nonlinear-regime with  $\delta_{LS} \gg 1$ , the significance of this link diminishes.
- The properties of the galaxies are also found to be linked to the types of the large-scale structure where they are embedded, even when the  $r$ -band absolute magnitude is constrained to a narrow range. The halo galaxies tend to have highest mean values of  $D(4000)$  and surface stellar mass density, while the void galaxies have lowest mean values of  $D(4000)$  and surface stellar mass density. For the filament galaxies, the mean values are found to be similar to the global mean averaged over the whole sample.

Our results have suggested that the galaxy-environment correlations are induced not only by the evolutionary processes like galaxy merging and interactions, but also by the initial cosmological conditions. Since galaxies are distributed on the largest scale in a tidally induced filamentary cosmic web, the large-scale tidal field is likely to affect the galaxy properties and link them to the shear of large-scale environment. This initially induced galaxy-environment link, however, is apt to be overwhelmed and superseded by the small-scale nonlinear processes especially in rich environments.

This work has had to be limited to low redshift galaxies ( $z \leq 0.04$ ), because of a similar redshift limit of the 2Mass Redshift Survey from which the real-space tidal field was constructed. To understand the true role of the large-scale shears in establishing the variations of galaxy properties, it will be necessary to reconstruct the tidal field at higher redshifts and investigate the evolution of the variations of the galaxy properties with the large-scale shears. Another limitation of the current work is that, because of the small size of the sample, the subsamples at “fixed” luminosity or overdensity still cover a relatively wide range of luminosity or overdensity, and so the correlation of luminosity with overdensity can not be completely removed when analyzing the other physical properties. We plan to reconstruct the real-space density and shear fields with the SDSS data, and hopefully we will be able to make significant progress with the new data.

A final conclusion is that our results may provide a new

insight into the galaxy formation in a cosmic web, which is still shrouded in mystery.

## ACKNOWLEDGMENTS

J.L. thank P. Erdogdu very much for providing the 2MRS density field. J.L. is also very grateful to the warm hospitality of S.D.M. White and the Max Planck Institute for Astrophysics (MPA) in Garching where this work was initiated and performed. J.L. is supported by the visiting scientist fellowship from MPA in Garching and the Korea Science and Engineering Foundation (KOSEF) grant funded by the Korean Government (MOST, NO. R01-2007-000-10246-0). C.L. is supported by the Joint Postdoctoral Programme in Astrophysical Cosmology of Max Planck Institute for Astrophysics and Shanghai Astronomical Observatory, and by NSFC (10533030, 10643005, 10633020) and 973 Program (No.2007CB815402).

Funding for the SDSS and SDSS-II has been provided by the Alfred P. Sloan Foundation, the Participating Institutions, the National Science Foundation, the U.S. Department of Energy, the National Aeronautics and Space Administration, the Japanese Monbukagakusho, the Max Planck Society, and the Higher Education Funding Council for England. The SDSS Web Site is <http://www.sdss.org/>. The SDSS is managed by the Astrophysical Research Consortium for the Participating Institutions. The Participating Institutions are the American Museum of Natural History, Astrophysical Institute Potsdam, University of Basel, Cambridge University, Case Western Reserve University, University of Chicago, Drexel University, Fermilab, the Institute for Advanced Study, the Japan Participation Group, Johns Hopkins University, the Joint Institute for Nuclear Astrophysics, the Kavli Institute for Particle Astrophysics and Cosmology, the Korean Scientist Group, the Chinese Academy of Sciences (LAMOST), Los Alamos National Laboratory, the Max-Planck-Institute for Astronomy (MPIA), the Max-Planck-Institute for Astrophysics (MPA), New Mexico State University, Ohio State University, University of Pittsburgh, University of Portsmouth, Princeton University, the United States Naval Observatory, and the University of Washington.

## REFERENCES

- Adelman-McCarthy J. K., Agüeros M. A., Allam S. S., Anderson K. S. J., Anderson S. F., Annis J., Bahcall N. A., Baldry I. K., et al., 2006, *ApJS*, 162, 38
- Balogh M. L., Morris S. L., Yee H. K. C., Carlberg R. G., Ellingson E., 1999, *ApJ*, 527, 54
- Balogh M. L., Christlein D., Zabludoff A. I., Zaritsky D., 2001, *ApJ*, 557, 117
- Bardeen J. M., Bond J. R., Kaiser N., Szalay A. S., 1986, *ApJ*, 304, 15
- Blanton M. R., Brinkmann J., Csabai I., Doi M., Eisenstein D., Fukugita M., Gunn J. E., Hogg D. W., et al., 2003a, *AJ*, 125, 2348
- Blanton M. R., Hogg D. W., Bahcall N. A., Brinkmann J., Britton M., Connolly A. J., Csabai I., Fukugita M., et al., 2003b, *ApJ*, 592, 819

- Blanton M. R., Lin H., Lupton R. H., Maley F. M., Young N., Zehavi I., Loveday J., 2003c, *AJ*, 125, 2276
- Blanton M. R., Eisenstein D., Hogg D. W., Schlegel D. J., Brinkmann J., 2005, *ApJ*, 629, 143
- Bond J. R., Kofman L., & Pogosyan D., 1996, *Nature*, 380, 603
- Brinchmann J., Charlot S., White S. D. M., Tremonti C., Kauffmann G., Heckman T., Brinkmann J., 2004, *MNRAS*, 351, 1151
- Budavári T., et al. , 2003, *ApJ*, 595, 59
- Davis M., Geller M. J., 1976, *ApJ*, 208, 13
- Dressler, A., 1980, *ApJ*, 236, 351
- Eisenstein, D. J. et al. 2001, *AJ*, 122, 2267
- Erdogdu P., Lahav O., Huchra J. P., Colless M., Cutri R. M., Falco E., George, T., Jarrett T., Jones D. H., Macri L. M., Mader J., Martimbeau N., Pahre M. A., Parker Q. A., Rassat A., Saunders W., 2006, *MNRAS*, 373, 45
- Fukugita M., Ichikawa T., Gunn J. E., Doi M., Shimasaku K., Schneider D. P., 1996, *AJ*, 111, 1748
- Gómez P. L., Nichol R. C., Miller C. J., Balogh M. L., Goto T., Zabludoff A. I., Romer A. K., Bernardi M., Sheth R., Hopkins A. M., Castander F. J., Connolly A. J., Schneider D. P., Brinkmann J., Lamb D. Q., SubbaRao M., York D. G., 2003, *ApJ*, 584, 210
- Goto T., Yamauchi C., Fujita Y., Okamura S., Sekiguchi M., Smail I., Bernardi M., Gomez P. L., 2003, *MNRAS*, 346, 601
- Gunn J. E., Carr M., Rockosi C., Sekiguchi M., Berry K., Elms B., de Haas E., Ivezić Ž., et al., 1998, *AJ*, 116, 3040
- Gunn J. E., Siegmund W. A., Mannery E. J., Owen R. E., Hull C. L., Leger R. F., Carey L. N., Knapp G. R., et al., 2006, *AJ*, 131, 2332
- Hogg D. W., Finkbeiner D. P., Schlegel D. J., Gunn J. E., 2001, *AJ*, 122, 2129
- Hogg D. W., et al., 2003, *ApJ*, 585, L5
- Ivezić Ž., Lupton R. H., Schlegel D., Boroski B., Adelman-McCarthy J., Yanny B., Kent S., Stoughton C., et al., 2004, *Astronomische Nachrichten*, 325, 583
- Kauffmann G., et al. , 2003, *MNRAS*, 341, 54
- Kauffmann G., White S. D. M., Heckman T. M., Ménard B., Brinchmann J., Charlot S., Tremonti C., Brinkmann J., 2004, *MNRAS*, 353, 713
- Lee J., Erdogdu P., 2007, *ApJ*, 671, 1248L
- Lee J., Lee B. 2008, *ArXiv Astrophysics e-prints*
- Lewis I., Balogh M., De Propris R. Couch W., Bower R., Offer, A., Bland-Hawthorn J., Baldry I. K., Baugh C., Bridges T., Cannon R., Cole, S., Colless M., Collins C., Cross N., Dalton G., Driver S. P., Efstathiou G. and Ellis R. S. and Frenk C. S., Glazebrook K., Hawkins E., Jackson C., Lahav O., Lumsden S., Maddox S., Madgwick D., Norberg P., Peacock J. A., Percival W., Peterson B. A., Sutherland W. & Taylor, K. 2002, *MNRAS*, 334, 673L
- Li C., Kauffmann G., Jing Y. P., White S. D. M., Börner G., Cheng F. Z., 2006, *MNRAS*, 368, 21
- Lupton R., Gunn J. E., Ivezić Z., Knapp G. R., Kent S., 2001, in Harnden Jr. F. R., Primi F. A., Payne H., eds, *Astronomical Data Analysis Software and Systems X Vol. 238, The SDSS Imaging Pipelines*. pp 269–+
- Madgwick D. S., et al. , 2003, *MNRAS*, 344, 847
- Martínez H. J., Zandivarez A., Domínguez M., Merchán M. E., Lambas D. G., 2002, *MNRAS*, 333, L31
- Mo H. J., McGaugh S. S., Bothun G. D., 1994, *MNRAS*, 267, 129
- Norberg, P., et al. 2001, *MNRAS*, 328, 64
- Norberg, P., et al. 2002, *MNRAS*, 332, 827
- Oemler A. J., 1974, *ApJ*, 194, 1
- Park C., Vogeley M. S., Geller M. J., Huchra J. P., 1994, *ApJ*, 431, 569
- Park C., Choi Y.-Y., Vogeley M. S., Gott J. R. I., Blanton M. R., 2007, *ApJ*, 658, 898
- Pier J. R., Munn J. A., Hindsley R. B., Hennessy G. S., Kent S. M., Lupton R. H., Ivezić Ž., 2003, *AJ*, 125, 1559
- Postman M., & Geller M. J., 1984, *ApJ*, 281, 95
- Richards, G. T. et al. 2002, *AJ*, 123, 2945
- Rojas R. R., Vogeley M. S., Hoyle F., Brinkmann J., 2005, *ApJ*, 624, 571
- Schlegel D. J., Finkbeiner D. P., Davis M., 1998, *ApJ*, 500, 525
- Smith J. A., Tucker D. L., Kent S., Richmond M. W., Fukugita M., Ichikawa T., Ichikawa S.-i., Jorgensen A. M., et al., 2002, *AJ*, 123, 2121
- Stoughton C., Lupton R. H., Bernardi M., Blanton M. R., Burles S., Castander F. J., Connolly A. J., Eisenstein D. J., et al., 2002, *AJ*, 123, 485
- Strauss M. A., Weinberg D. H., Lupton R. H., Narayanan V. K., Annis J., Bernardi M., Blanton M., Burles S., et al., 2002, *AJ*, 124, 1810
- Tanaka M., Goto T., Okamura S., Shimasaku K., & Brinkman J., 2004, *AJ*, 128, 2677
- Tucker D. L., Kent S., Richmond M. W., Annis J., Smith J. A., Allam S. S., Rodgers C. T., Stute J. L., et al., 2006, *Astronomische Nachrichten*, 327, 821
- Whitmore B. C. Gilmore D. M. & Jones C., 1993, *ApJ*, 407, 489
- York D. G., Adelman J., Anderson Jr. J. E., Anderson S. F., Annis J., Bahcall N. A., Bakken J. A., Barkhouser R., et al., 2000, *AJ*, 120, 1579
- Zehavi, I., et al. 2002, *ApJ*, 571, 172
- Zehavi I., et al., 2005, *ApJ*, 630, 1

This paper has been typeset from a  $\text{\TeX}$ / $\text{\LaTeX}$  file prepared by the author.